Available online at www.sciencedirect.com

ScienceDirect

journal homepage: www.elsevier.com/locate/he

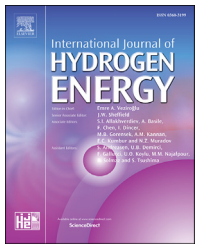

A new catalyst of AlCu@ZnO for hydrogen evolution reaction

Bulut Hüner [a], *Murat Farsak* [b], *Esra Telli* [a,*]

[a] *Osmaniye Korkut Ata University, Engineering Faculty, Energy Systems Engineering Faculty, Osmaniye, Turkey*
[b] *Osmaniye Korkut Ata University, Applied Science School of Kadirli, Food Technology, Osmaniye, Turkey*

ARTICLE INFO

Article history:
Received 22 January 2018
Received in revised form
26 February 2018
Accepted 28 February 2018
Available online 22 March 2018

Keywords:
ZnO
Sol-gel
Aluminum
Copper

ABSTRACT

Thin films of undoped ZnO, Al-doped ZnO, Cu-doped ZnO, and AlCu@ZnO deposited on indium tin oxide were performed by the sol-gel spin coating method. The prepared ZnO thin films were investigated for their structural and electrical properties after annealing at 500 °C for 1 h. ZnO thin films were characterized by electrochemical impedance spectroscopy, linear sweep voltammetry, scanning electron microscopy, Fourier transform infrared spectroscopy and Mott Schottky. According to the results obtained from the Nyquist diagrams of the ZnO thin films, the resistance value was found to decrease with binary doping and the resistance value was found to be lowest in AlCu@ZnO doped thin film containing 0.01 M Al and 0.1 M Cu. As ZnO thin films go to cathodic potentials, it is seen that the cathodic current value of ZnO with undoped is the lowest. It has been found that only Al and Cu doping showed less cathodic current than double doping.

Introduction

Hydrogen energy systems are seen as one of the most effective solutions, playing an important role in terms of environment and sustainability [1]. Hydrogen is a sustainable fuel and one of the most promising potential solutions to energy and the environment for problems that exist in the world [2]. Recently, there has been a growing interest in the new method of preventing greenhouse gases from fossil fuel consumption and producing hydrogen from renewable energy sources [3]. Several studies have been conducted in literature related to hydrogen production using different methods [4–9]. Hydrogen is usually produced from fossil fuels and approximately 96% of the hydrogen is formed by steam reforming of the natural gas. The remaining 4% is produced by water electrolysis. Water electrolysis can be a promising method for obtaining hydrogen in the future [10,11]. Another way to improve research and development in water electrolysis is to reduce the cost of investment and to increase technological efficiency. There is a lot of work on the subject of water electrolysis, and most of them focus on the development of factors such as temperature, pressure, electrode materials and catalyst [12,13]. Water electrolysis is now used for hydrogen production from renewable energy sources due to its high energy efficiency [14]. Hydrogen production by solar energy in water electrolysis usually takes place in three ways: Thermochemical electrolysis of water, photobiologically electrolysis of water and photocatalytic electrolysis of water. Electrolysis of water photocatalytically is a promising technology to produce "clean" hydrogen. Photocatalytics are defined as a chemical reaction induced by photon irradiation in the presence of a catalyst, or in particular a photocatalyst. Photocatalysts play an important role in the electrolysis

* *Corresponding author.*
E-mail addresses: hunerbulut@gmail.com (B. Hüner), muratfarsak@osmaniye.edu.tr (M. Farsak), esratelli@osmaniye.edu.tr (E. Telli).
https://doi.org/10.1016/j.ijhydene.2018.02.186

reaction of photocatalytic water [15]. Catalysts used in photocatalytic reactions are always semiconducting materials. These materials include several metal oxides such as TiO_2 [16], CeO_2, ZnO [17,18], WO_3 [19], Fe_2O_3 [20], Cu-Al [21], and even sulfides such as CdS [22], ZnS [23], MoS_2 [24]. In addition, C/CoSnZn-Pd, NiCu/C, NiCoZn-M, NiMn, GaN, and Cu/SiO_2 can be used as the electrocatalyst in hydrogen production [25–30]. Although metal oxides in most of the applications are fewer catalysts than noble metals, metal oxides are more resistant to deactivation. Furthermore, the incorporation of two or more metal oxide catalysts can improve catalytic activity [31]. In particular, zinc oxide (ZnO) has a significant effect on photocatalytic applications due to its low cost, non-toxic and high quantum yields [32].

ZnO belonging to group II-VI is a semiconducting material with high transmittance in the visible region with a wide band gap [33]. It has potential applications for ZnO optoelectronic devices at 3.37 eV at room temperature and 3.44 eV wide band at low temperature [34]. ZnO has a hexagonal wurtzite structure and for this structure, the braid constants a = 3.25 Å, c = 5.12 Å. It is known that the hexagonal wurtzite ZnO films have (002) preferential orientation along the c-axis [35]. Undoped ZnO thin films show n-type conductivities due to defects such as oxygen vacancies. Doped thin films are obtained by using additive such as Al and Cu [36]. Transparent and conductive Al-doped ZnO thin films are widely used in various optoelectronic applications such as solar cells and organic light emitting diodes [37]. It has been shown that the electrical properties of the zinc oxide thin films can be clearly improved by doping with Al [38]. ZnO thin films have been shown to change their electrical properties when Cu doping is performed. Semiconductor properties such as conductivity and carrier concentration have been changed depending on the amount of doping Cu [39]. ZnO thin films can be obtained using many different methods such as DC magnetron sputtering [37,40], electrodeposition [38], ultrasonic spray pyrolysis [41,42], sol-gel method [43,44], and pulsed laser deposition [45]. Among these methods, the sol-gel method has many advantages: simplicity, low-cost, low-temperature operation, easy processing of samples, suitable for the production of films in small and large areas for industrial applications [46].

In this article, semiconductor electrodes were prepared by doping aluminum and/or copper on ZnO prepared by sol-gel technique. The structural and electrical properties of the obtained films were investigated using Electrochemical Impedance Spectroscopy (EIS), Linear Sweep Voltammetry (LSV), Scanning Electron Microscopy (SEM), Fourier Transform Infrared Spectroscopy (FTIR) and Mott Schottky (MS).

Experimental

Indium tin oxide (ITO) was used in the experiments as substrate. The substrate surface area was used as 2 cm^2. ITOs (surface resistivity: < 10 Ω) were cleaned respectively in detergent, acetone, and isopropyl alcohol for 10 min each by using an ultrasonic cleaner and then cleaned with deionized water and dried.

ZnO thin films have been deposited by the sol-gel spin coating method on ITOs. As a starting material and dopant sources, zinc acetate dihydrate [$Zn(CH_3COO)_2 \cdot 2H_2O$], aluminum chloride hexahydrate [$AlCl_3 \cdot 6H_2O$] and copper (II) chloride dihydrate [$CuCl_2 \cdot 2H_2O$] were used. In the preparation of the solution, 20 mL aqueous solution of 0.5 M zinc acetate was prepared. Then, 50 mL of mono ethanolamine (MEA) was added as stabilizer, 0.1 M $AlCl_3 \cdot 6H_2O$ and 0.1 M $CuCl_2 \cdot 2H_2O$ dissolved in 10 mL of ethanol were added to the solution, and the mixture solution was stirred in a water bath for 1 h at 60 °C. 6 mL of concentrated ammonium hydroxide was added in the mixture solution and the mixture also was stirred at 60 °C for 10 min, after 10 mL purified water was added to the mixture. Then, a light yellowish clear solution was obtained and aged at room temperature for 24 h statically. Fig. 1 shows the flow chart of ZnO films prepared by sol-gel technique. The

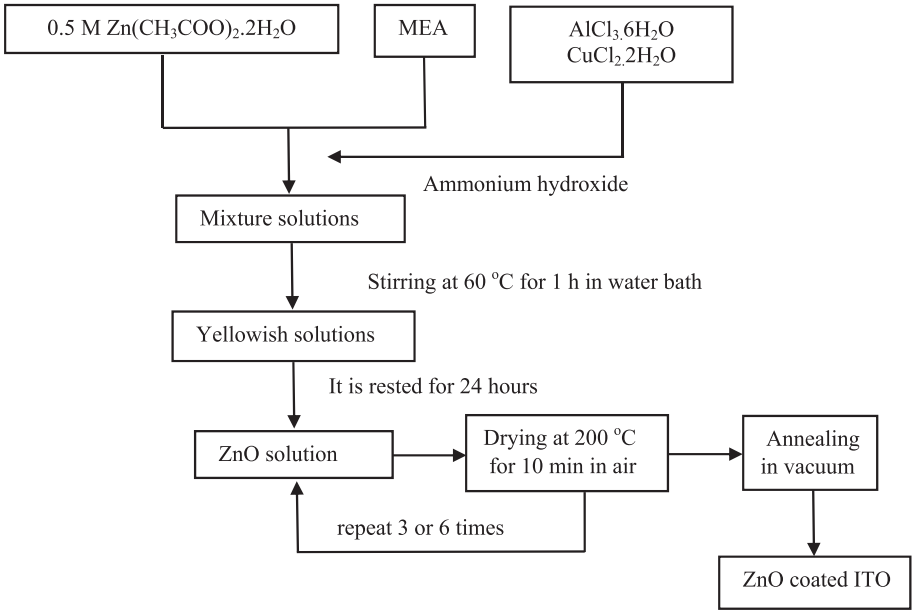

Fig. 1 – Flow chart of ZnO films prepared by sol-gel technique.

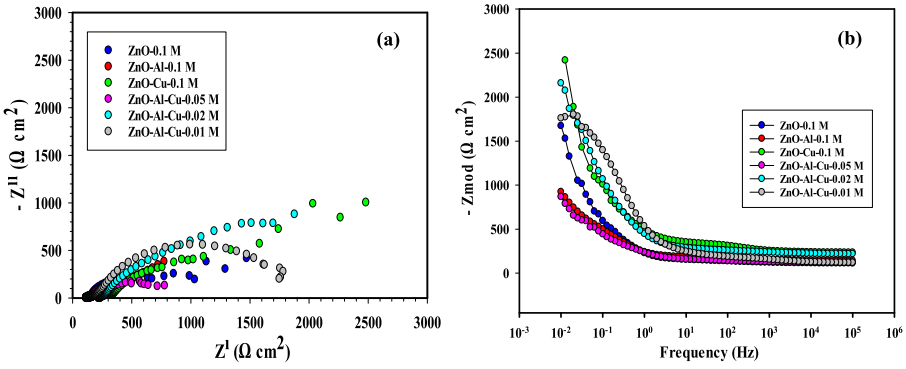

Fig. 2 – (a) Nyquist diagram and (b) Bode diagram of undoped ZnO, Al and Cu doped ZnO analyzed in the dark at OCP.

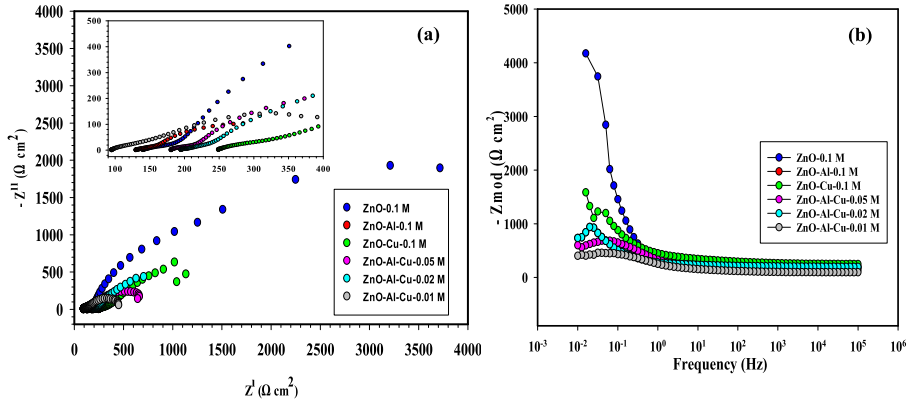

Fig. 3 – (a) Nyquist diagram and (b) Bode diagram of undoped ZnO, Al and Cu doped ZnO analyzed under 100 W light at OCP.

Table 1 – Resistance values and efficiency (%) values of electrodes.

The name of the electrodes	In the dark Ω cm^2	Efficiency (%)	Under 100 W light Ω cm^2	Efficiency (%)
Undoped ZnO	1471.8	– – –	3720.0	– – –
Al-doped ZnO	774.6	47.4	452.6	87.8
Cu-doped ZnO	2482.0	– – –	1043.6	71.9
0.05 M AlCu@ZnO	778.4	47.1	647.2	82.6
0.02 M AlCu@ZnO	1877.6	– – –	706.2	81.0
0.01 M AlCu@ZnO	1749.2	– – –	371.4	90.0

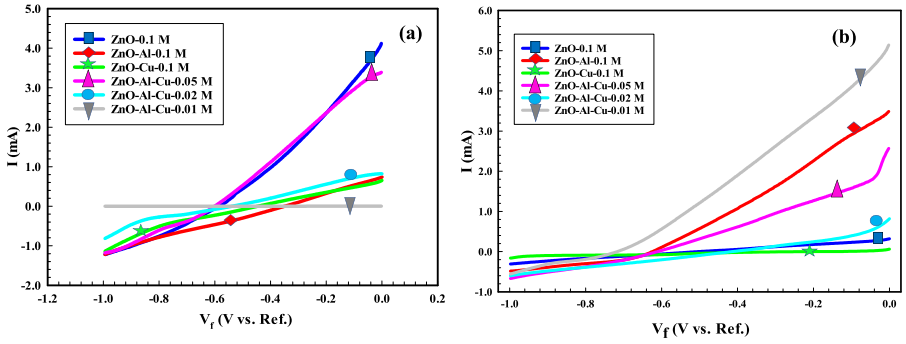

Fig. 4 – (a) In the dark, (b) under 100 W light, LSV diagram of undoped ZnO, Al and Cu doped ZnO.

prepared ZnO solution was deposited on ITO with the spin coating method (Laurell Tech. Cor. WS-650MZ-23NPPB) (at 600 rpm for 30 s) and pre–dried at 200 °C for 10 min with air. This process was repeated 3 or 6 times. After pre–drying, the ITOs were vacuum annealed at 500 °C for 1 h.

EIS, LSV, SEM, FTIR and MS analyzes

ZnO thin films were analyzed by examining the dark and under 100 Watt light. The electrochemical properties of the ZnO thin films were analyzed by using LSV, EIS and MS techniques. EIS measurements were analyzed at a frequency range from 100 kHz to 0.01 Hz at an amplitude of 5 mV. All EIS analysis were performed at open circuit potential (OCP). LSV measurements were investigated with a scan rate of 5 mV/s. The electrochemical characterization techniques were performed using potentiostat–galvanostat (Gamry Interface 1000) by three-electrode technique. EIS, LSV and MS measurements were analyzed in 0.1 M KCl solution using Pt as the reference and counter electrode. The platinum electrode used as the reference electrode is arranged according to the reference electrode Ag/AgCl. The structural properties of the obtained films were investigated using SEM (FEI Quanta 650 Field Emission SEM) and FTIR (Perkin Elmer Spectrum 65).

Results and discussion

Figs. 2 and 3 show the Nyquist diagram (a) and bode diagram (b) of undoped ZnO (0.1 M), Al doped ZnO (0.1 M) and Cu doped ZnO (0.1 M) at OCP. As shown in Fig. 2, it is seen that highest resistance (2500 Ω cm^2) of thin films belong to the Cu doped ZnO (0.1 M) of the thin film analyzed in the dark. In Fig. 3, it is observed that the resistivity (4000 Ω cm^2) has the highest value in the ZnO thin film which is analyzed under 100 W light and that this resistance value decreases with the ZnO doped. When only Al and Cu are doped, the resistance is reduced to some extent while the lowest resistance is also seen in binary doped ZnO containing 0.01 M Al and 0.1 M Cu. It is known from the volcano curve that the ability of copper hydrogen desorption is high [47]. Copper coating on ZnO appears to enhance hydrogen evolution activity. The doping of impurities such as Al, In, Ga and B resulted in high electrical conductivity [48]. For this reason, it is seen that the lowest resistance is Al and Cu doped ZnO.

Table 2 – Cathodic current values and efficiency (%) values of electrodes.

The name of the electrodes	In the dark	Under 100 W light	Efficiency (%)
Undoped ZnO	1.234 mA	0.308 mA	– – –
Al-doped ZnO	1.226 mA	0.485 mA	36
Cu-doped ZnO	1.160 mA	0.162 mA	−0.47
0.05 M AlCu@ZnO	1.179 mA	0.674 mA	54
0.02 M AlCu@ZnO	0.829 mA	0.601 mA	48
0.01 M AlCu@ZnO	0.568 mA	0.558 mA	45

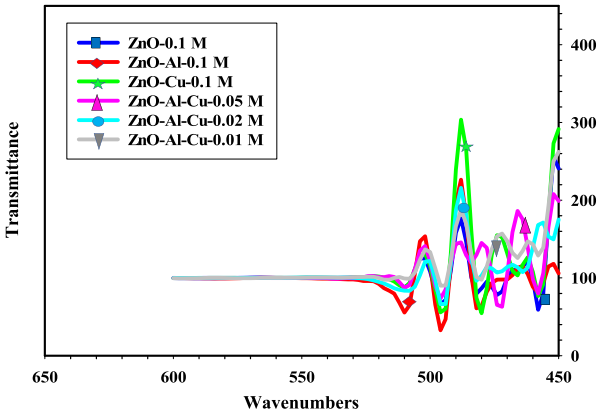

Fig. 6 – FTIR spectrum of ZnO, Al doped ZnO, Cu doped ZnO, AlCu@ZnO 0.01 M, AlCu@ZnO 0.02 M and AlCu@ZnO 0.05 M electrodes.

In Table 1, the resistance values and activities occurring as a result of EIS analysis under 100 W light and in the dark are given in percent (%).

Fig. 4 shows that LSV technique, the current potential curves of ZnO, Al-doped ZnO, Cu-doped ZnO and AlCu@ZnO 0.05 M, AlCu@ZnO 0.02 M and AlCu@ZnO 0.01 M thin films were investigated with a scan rate of 5 mV/s.

It is seen that the cathodic current value of the ZnO with no contribution to the cathodic potentials is the lowest, and an increase in the cathodic current value is observed with the doping. It was found that only Cu and Al doping showed less cathodic current than binary doping. In binary doping, the

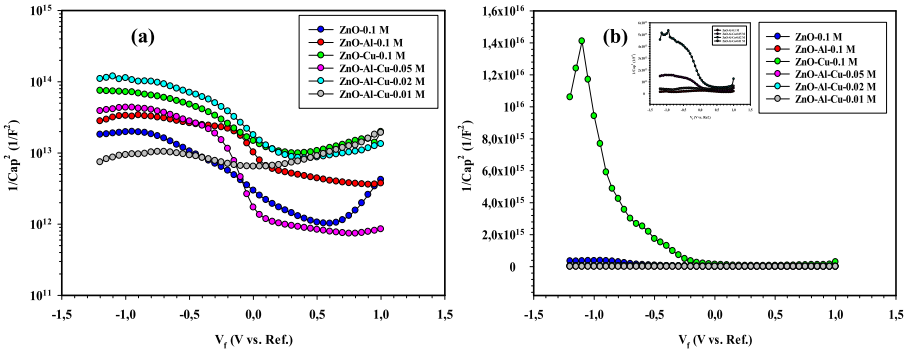

Fig. 5 – (a) In the dark, (b) under 100 W light, MS diagram of undoped ZnO, Al and Cu doped ZnO.

highest cathodic current value belongs to AlCu@ZnO 0.01 M. It is understood from this that AlCu@ZnO 0.01 M is the most efficient electrode for hydrogen production.

In Table 2, the cathodic current values and efficiencies generated as a result of LSV analysis under 100 W light and in the dark are given in percent (%).

MS measurements were analyzed in the dark and under 100 W of light and are shown in Fig. 5. MS measurements of the obtained ZnO thin films show that the electrodes are negatively inclined. The negative slope indicates that the electrodes are p-type semiconductors. The fact that the electrodes have a p-type semiconductor property is a desirable condition for the hydrogen obtained.

FTIR is a technique used to obtain information about chemical bonding in a material and is used to describe the basic components of a substance [49]. Infrared is the distinctive region for metals between frequencies 450 and 600. When we examine the infrared images of the electrodes in this region in Fig. 6, we see that each dopant differs from the other.

Fig. 7 shows the effects on the surface morphology of ZnO, Al-doped ZnO, Cu-doped ZnO and AlCu@ZnO (different concentrations) thin films. In Fig. 7 (a), undoped ZnO thin film has shown a clear stripe–like layered in the SEM micrograph. Fig. 7 (b)-(c) show that Al-doped and Cu-doped ZnO thin films have a hexagonal structure. After the deposition, the strip structure was transformed into a hexagonal structure. Fig. 7 (d)-(f) show that AlCu@ZnO films obtained forms hexagonally and depending on the increasing aluminum concentration, the surface morphologies of the films are changed. It is clearly seen that AlCu@ZnO 0.01 M has larger porosities than the other binary dopants. In 0.1 M Al-doped ZnO thin film, the particle size is 686.5 nm, whereas in 0.01 M Al and 0.1 M Cu doped ZnO thin film this ratio is 456.6 nm. As is known, the reduction of pore size increases the number of pores and thus

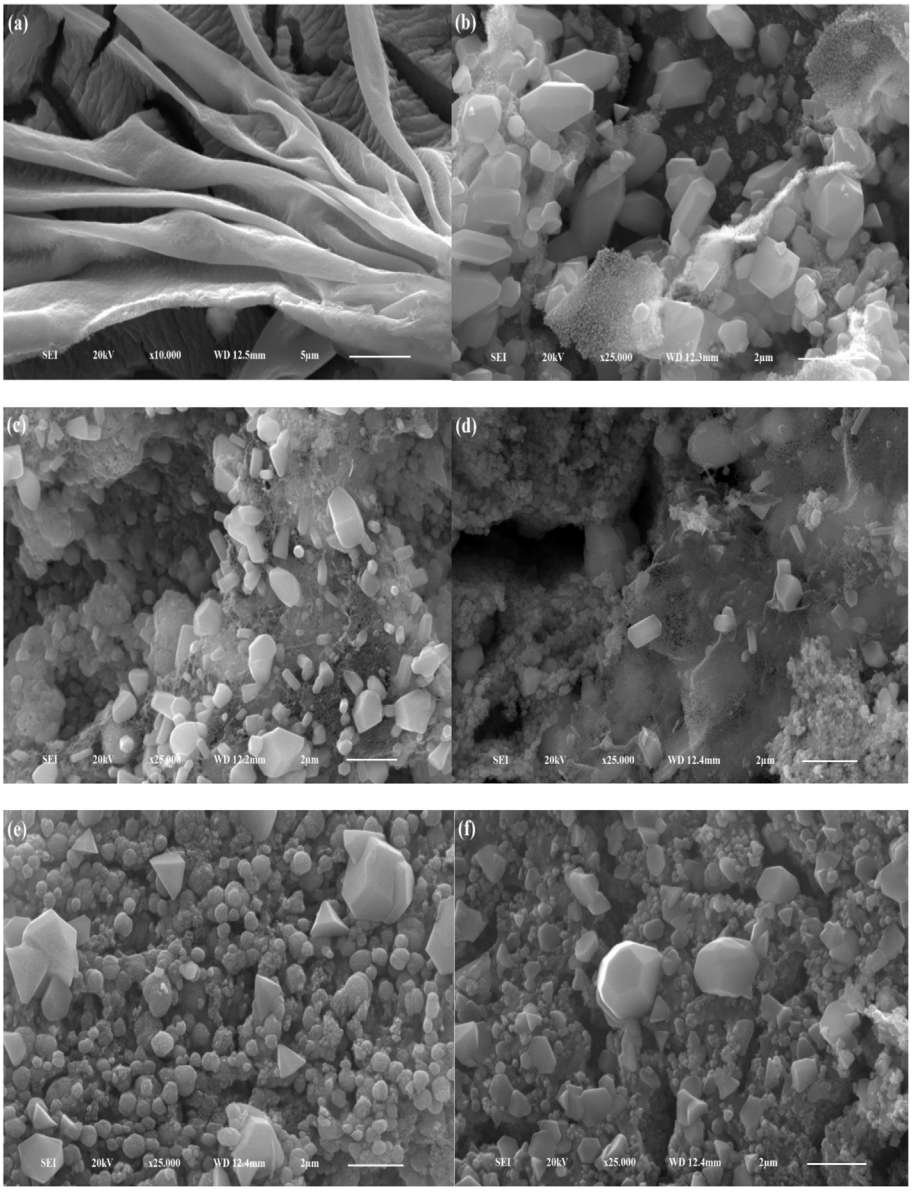

Fig. 7 – SEM images of (a) ZnO, (b) Al-doped ZnO, (c) Cu-doped ZnO, (d) AlCu@ZnO 0.01 M, (e) AlCu@ZnO 0.02 M and (f) AlCu@ZnO 0.05 M.

the surface area is also increasing. Increasing the surface area increases the number of active centers to which hydrogen molecules can attach. This explains why AlCu@ZnO 0.01 M is more catalytically active.

Conclusions

Undoped ZnO, Al-doped ZnO, Cu-doped ZnO, AlCu@ZnO 0.01 M, AlCu@ZnO 0.02 M, and AlCu@ZnO 0.05 M thin films were coated on ITO glass substrates by the sol-gel method. According to the results obtained from the Nyquist diagrams, it is seen that the resistance value decreases with binary doping and the resistance value is lowest in AlCu@ZnO 0.01 M. According to the results of LSV, in the binary doping the highest cathodic current value belongs to AlCu@ZnO 0.01 M. It is understood from this that AlCu@ZnO 0.01 M is the most efficient electrode for hydrogen production. According to SEM images, it has been observed that crystal structure change on the surface of films when the Al-doped ZnO concentration is increased up to 0.05 M from 0.01 M. Al doped ZnO and Cu doped ZnO have been observed to be more catalytic effective than undoped ZnO.

Acknowledgements

This study has been financially supported by Osmaniye Korkut Ata University research fund. The authors are greatly thankful to Osmaniye Korkut Ata University research fund (Project Number: OKÜBAP-2015-PT2-004) and Çukurova University. The authors would like to especially thank to Gülfeza Kardaş for help.

REFERENCES

[1] Dincer I. Green methods for hydrogen production. Int J Hydrogen Energy 2012;37:1954–71.
[2] Coskun C, Akyuz E, Oktay Z, Dincer I. Energy analysis of hydrogen production using biogas-based electricity. Int J Hydrogen Energy 2011;36:11418–24.
[3] Ahmad H, Kamarudin S, Minggu L, Kassim M. Hydrogen from photo-catalytic water splitting process: a review. Renew Sustain Energy Rev 2015;43:599–610.
[4] Sakr I, Abdelsalam AM, El-Askary W. Effect of electrodes separator-type on hydrogen production using solar energy. Energy 2017;140:625–32.
[5] Machín A, Cotto M, Duconge J, Arango JC, Morant C, Pinilla S, et al. Hydrogen production via water splitting using different Au@ ZnO catalysts under UV–vis irradiation. J Photochem Photobiol Chem 2018;353:385–94.
[6] Karakilcik M, Erden M, Cilogulları M, Dincer I. Investigation of hydrogen production performance of a reactor assisted by a solar pond via photoelectrochemical process. Int J Hydrogen Energy 2018 (in press).
[7] Çelik D, Yıldız M. Investigation of hydrogen production methods in accordance with green chemistry principles. Int J Hydrogen Energy 2017;42:23395–401.
[8] Döner A, Solmaz R, Kardaş G. Enhancement of hydrogen evolution at cobalt–zinc deposited graphite electrode in alkaline solution. Int J Hydrogen Energy 2011;36:7391–7.
[9] Solmaz R, Salcı A, Yüksel H, Doğrubaş M, Kardaş G. Preparation and characterization of Pd-modified Raney-type NiZn coatings and their application for alkaline water electrolysis. Int J Hydrogen Energy 2017;42:2464–75.
[10] Bičáková O, Straka P. Production of hydrogen from renewable resources and its effectiveness. Int J Hydrogen Energy 2012;37:11563–78.
[11] Nikolaidis P, Poullikkas A. A comparative overview of hydrogen production processes. Renew Sustain Energy Rev 2017;67:597–611.
[12] Dobó Z, Palotás ÁB. Impact of the current fluctuation on the efficiency of alkaline water electrolysis. Int J Hydrogen Energy 2017;42:5649–56.
[13] Sikander U, Sufian S, Salam M. A review of hydrotalcite based catalysts for hydrogen production systems. Int J Hydrogen Energy 2017;42:19851–68.
[14] Guo L, Zhao L, Jing D, Lu Y, Yang H, Bai B, et al. Reprint of: solar hydrogen production and its development in China. Energy 2010;35:4421–38.
[15] Liao C-H, Huang C-W, Wu J. Hydrogen production from semiconductor-based photocatalysis via water splitting. Catalysts 2012;2:490–516.
[16] Radecka M. TiO2 for photoelectrolytic decomposition of water. Thin Solid Films 2004;451:98–104.
[17] Tseng C-F, Hsu W-Y. Sol–gel derived ZnO–CeO2 thin films on glass substrate. Thin Solid Films 2013;544:44–7.
[18] Carrasco-Jaim OA, Ceballos-Sanchez O, Torres-Martínez LM, Moctezuma E, Gómez-Solís C. Synthesis and characterization of PbS/ZnO thin film for photocatalytic hydrogen production. J Photochem Photobiol Chem 2017;347:98–104.
[19] Madhukar P, Jyothi DS, Jayababu N, Reddy MR. Influence of annealing temperature on structural and dielectric properties of e-beam evaporated WO3 thin films. Mater Today Proc 2016;3:4199–204.
[20] Khan U, Akbar A, Yousaf H, Riaz S, Naseem S. Ferromagnetic properties of Al-doped Fe2O3 thin films by Sol-Gel. Mater Today Proc 2015;2:5415–20.
[21] Li G, Gu C, Zhu W, Wang X, Yuan X, Cui Z, et al. Hydrogen production from methanol decomposition using Cu-Al spinel catalysts. J Clean Prod 2018;183:415–23.
[22] Moualkia H, Hariech S, Aida M. Structural and optical properties of CdS thin films grown by chemical bath deposition. Thin Solid Films 2009;518:1259–62.
[23] Chang C-J, Wei Y-H, Huang K-P. Photocatalytic hydrogen production by flower-like graphene supported ZnS composite photocatalysts. Int J Hydrogen Energy 2017;42:23578–86.
[24] Molinarı R, Marino T, P A. Photocatalytic membrane reactors for hydrogen production from water. Int J Hydrogen Energy 2014:7247–61.
[25] Döner A, Tezcan F, Kardaş G. Electrocatalytic behavior of the Pd-modified electrocatalyst for hydrogen evolution. Int J Hydrogen Energy 2013;38:3881–8.
[26] Zhang H, Wang Y, Wu Z, Leung DY. An ammonia electrolytic cell with NiCu/C as anode catalyst for hydrogen production. Energy Procedia 2017;142:1539–44.
[27] Solmaz R, Kardaş G. Fabrication and characterization of NiCoZn–M (M: Ag, Pd and Pt) electrocatalysts as cathode materials for electrochemical hydrogen production. Int J Hydrogen Energy 2011;36:12079–87.
[28] Yüce AO, Döner A, Kardaş G. NiMn composite electrodes as cathode material for hydrogen evolution reaction in alkaline solution. Int J Hydrogen Energy 2013;38:4466–73.
[29] Suárez-Vázquez S, Limón-Pozos A, Campos-Badillo A, Fajardo G, Cruz-López A. Influence of electronic and optical properties of GaN nanoparticles as potential electrocatalyst in hydrogen production. Mater Sci Semicond Process 2017;64:124–9.

[30] Roselin LS, Chiu H-W. Production of hydrogen by oxidative steam reforming of methanol over Cu/SiO2 catalysts. Journal of Saudi Chemical Society 2017 (in press).
[31] Ibhadon AO, Fitzpatrick P. Heterogeneous photocatalysis: recent advances and applications. Catalysts 2013;3:189–218.
[32] Xia Y, Wang J, Chen R, Zhou D, Xiang L. A review on the fabrication of hierarchical ZnO nanostructures for photocatalysis application. Crystals 2016;6:148.
[33] Mahroug A, Boudjadar S, Hamrit S, Guerbous L. Structural, optical and photocurrent properties of undoped and Al-doped ZnO thin films deposited by sol–gel spin coating technique. Mater Lett 2014;134:248–51.
[34] Ismail AH, Abdullah AH, Sulaiman Y. Physical and electrochemical properties of ZnO films fabricated from highly cathodic electrodeposition potentials. Superlattice Microst 2017;103:171–9.
[35] Wang M, Lee KE, Hahn SH, Kim EJ, Kim S, Chung JS, et al. Optical and photoluminescent properties of sol-gel Al-doped ZnO thin films. Mater Lett 2007;61:1118–21.
[36] Baba K, Lazzaroni C, Nikravech M. ZnO and Al doped ZnO thin films deposited by Spray Plasma: effect of the growth time and Al doping on microstructural, optical and electrical properties. Thin Solid Films 2015;595:129–35.
[37] Kang D-W, Kuk S-H, Ji K-S, Lee H-M, Han M-K. Effects of ITO precursor thickness on transparent conductive Al doped ZnO film for solar cell applications. Sol Energy Mater Sol Cell 2011;95:138–41.
[38] Henni A, Merrouche A, Telli L, Karar A. Studies on the structural, morphological, optical and electrical properties of Al-doped ZnO nanorods prepared by electrochemical deposition. J Electroanal Chem 2016;763:149–54.
[39] Liau LC-K, Huang J-S. Energy-level variations of Cu-doped ZnO fabricated through sol-gel processing. J Alloy Comp 2017;702:153–60.
[40] Makino H, Shimizu H. Influence of crystallographic polarity on the opto-electrical properties of polycrystalline ZnO thin films deposited by magnetron sputtering. Appl Surf Sci 2018;439:839–44.
[41] Gahtar A, Rahal A, Benhaoua B, Benramache S. A comparative study on structural and optical properties of ZnO and Al-doped ZnO thin films obtained by ultrasonic spray method using different solvents. Optik-Int J Light Electron Optic 2014;125:3674–8.
[42] Mata V, Maldonado A, de la Luz Olvera M. Deposition of ZnO thin films by ultrasonic spray pyrolysis technique. Effect of the milling speed and time and its application in photocatalysis. Mater Sci Semicond Process 2018;75:288–95.
[43] Thirumoorthi M, Prakash JTJ. Structural, morphological characteristics and optical properties of Y doped ZnO thin films by sol–gel spin coating method. Superlattice Microst 2015;85:237–47.
[44] Nasser R, Elhouichet H. Production of acceptor complexes in sol-gel ZnO thin films by Sb doping. J Lumin 2018;196:11–9.
[45] Vakulov Z, Zamburg E, Khakhulin D, Ageev O. Thermal stability of ZnO thin films fabricated by pulsed laser deposition. Mater Sci Semicond Process 2017;66:21–5.
[46] Li J, Xu J, Xu Q, Fang G. Preparation and characterization of Al doped ZnO thin films by sol–gel process. J Alloy Compd 2012;542:151–6.
[47] Solmaz R, Kardaş G. Hydrogen evolution and corrosion performance of NiZn coatings. Energy Convers Manag 2007;48:583–91.
[48] Kim Y-S, Tai W-P. Electrical and optical properties of Al-doped ZnO thin films by sol–gel process. Appl Surf Sci 2007;253:4911–6.
[49] Muthukumaran S, Gopalakrishnan R. Structural, FTIR and photoluminescence studies of Cu doped ZnO nanopowders by co-precipitation method. Opt Mater 2012;34:1946–53.